Mapping the Number of Fibre Orientations per Voxel in Diffusion MRI

S. Nedjati-Gilani[1], G. J. Parker[2], D. C. Alexander[1]

[1]Centre for Medical Image Computing (CMIC), University College London, London, United Kingdom, [2]Imaging Science and Biomedical Imaging, University of Manchester, Manchester, United Kingdom

INTRODUCTION The aim of this work is to map the number of fibre populations in each voxel of a 3D diffusion MRI acquisition. We present a computationally expensive and accurate model generation and selection algorithm. We compare results from this new method with those obtained from an existing algorithm, and show that the new method provides denser clusters of fibre-crossing voxels, which suggests more reliable identification.

METHOD We generate the map by fitting a hierarchy of models of the particle displacement density, with increasing numbers of distinct fibre populations, to the diffusion MRI measurements in each voxel. We select the simplest model that describes the data in each voxel. The hierarchy of models are in the form proposed by [4], $A^*(\mathbf{q}) = A^*(\mathbf{0})\left(\left(1-\sum_{n=1}^{N} f_n\right)\exp\left(-t|\mathbf{q}|^2 d\right)+\sum_{n=1}^{N} f_n \exp\left(-td(\mathbf{e}_n\cdot\mathbf{q})^2\right)\right)$, where $A^*(\mathbf{q})$ is the unnormalised measurement at wavenumber $\mathbf{q}$, $A^*(\mathbf{0})$ is the signal with no diffusion-weighting coefficients, $\mathbf{e}_n$ is a unit vector in the direction of the nth fibre population, N is the number of fibre populations, d is the apparent diffusion coefficient, and f_n is the volume fraction of the nth fibre. We use a Levenberg-Marquardt algorithm to fit the models in the above equations to the data for N = 0, 1, 2, 3 by least-squares minimisation. The fitting process provides estimates of d, $A^*(\mathbf{0})$, f_n and $\mathbf{e}_n$. The Levenberg-Marquardt algorithm does not guarantee to find the global minimum of the objective function. In order to improve the chances of finding the global minimum, we run the fitting routine many times from perturbed starting points, created by additive Gaussian noise for $A^*(\mathbf{0})$, f_n, d and $\mathbf{e}_n$. The repeated runs determine the fraction of trials in which the fitting routine finds the global minimum or a value to within 0.1% of the global minimum, and thus determine the probability of finding the global minimum in a single run. These probabilities provide an estimate of the number of runs required to find the global minimum to some degree of confidence in each voxel. We compute the number of runs required separately for each model in the hierarchy. We assume the runs that produce the smallest fitting error find the global minimum. In practice, for voxels where the minimum is located only once in the repeated runs, we assume the minimum has not been found.

In order to decide the most suitable model for each voxel, the results obtained from each model must be compared with one another. We use an F-test [5] to select the best model for the data in each voxel. The F-test compares two nested models to decide whether the improvement of fit from the more complicated model is worth the cost of including the additional variables.

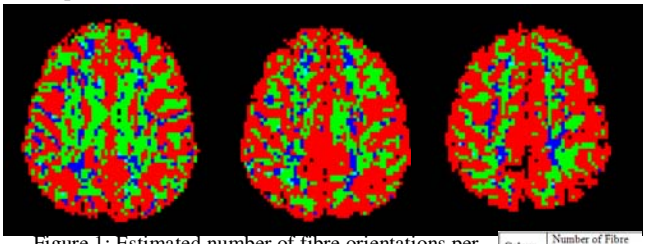

Figure 1: Estimated number of fibre orientations per voxel for three slices of a brain.

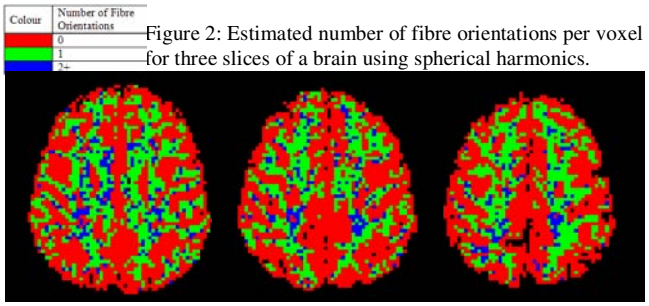

Figure 2: Estimated number of fibre orientations per voxel for three slices of a brain using spherical harmonics.

RESULTS The results suggest that for each voxel, we can find the global minimum at least once with 95% certainty for N = 0, 1, 2, 3 fibre orientations using 4, 15, 45 and 1626 runs of the Levenberg-Marquardt algorithm respectively. To reduce computation time, we limit the N = 3 case to 162 runs, which provides a 90% chance of finding the global minimum. We run the model fitting and selection procedure in each voxel of a 128×128×10 image with 61 diffusion weighted images with a b-value of 1270 s mm^{-2} and eight measurements at $\mathbf{q} = \mathbf{0}$, producing the results shown in Figure 1. For comparison, we show results from using spherical harmonics as a voxel classification algorithm [6] on the same slices in Figure 2. The results are similar in both cases in terms of differentiating areas of isotropic and anisotropic diffusion. The results of the new technique however tend to show a less dispersed distribution of 2-fibre voxels, and also has the benefit of distinguishing between 2-fibre and 3-fibre voxels. Table 1 provides a comparison of the two methods based on the number of isolated voxels using 6-connectivity to decide adjacency of voxels. Some 2-fibre clusters appear in different locations. The spherical harmonics-based method looks for non-Gaussian diffusion rather than distinct fibres specifically, and so may be sensitive to different microstructural architecture.

Table 1	I = Number of isolated voxels			T = Total number of voxels in class			I/T		
No of fibre-orientations	0	1	2+	0	1	2+	0	1	2+
New method	89	218	394	13067	7491	2058	0.68%	2.91%	19.15%
Spherical Harmonics	96	208	553	12778	7775	2063	0.75%	2.68%	26.81%

DISCUSSION AND CONCLUSION We have suggested a method for mapping the number of fibre orientations in each voxel of a 3D diffusion MRI acquisition. This information can be used for selecting the most appropriate algorithm for finding the orientations of fibres in each voxel. The approach described does have some limitations, as it does not allow for oblate fibre orientation distributions, which could be expected in various brain regions in the presence of fanning (e.g. corona radiata) and of high curvature (e.g. optic radiation). The results generated from this method share similarities to those obtained using the method described by Alexander et al [6], as can be seen by comparing the images shown above, and by comparing the distribution of isolated voxels. The spherical harmonic method provides a more dispersed distribution of voxels containing 2+ fibre orientations, which may indicate that a higher fraction of these voxels are classified as such due to noise. We might improve our method by using global optimization techniques such as simulated annealing for fitting. The new method is computationally expensive, but we plan to use the output as a 'gold standard' for simpler and faster ways of mapping the number of distinct fibre populations.

REFERENCES 1. Basser P.J. *et al, J Magn Reson B* 1996;111:209-219. 2. Jansons K.M. *et al, Inverse Problems* 2003;19:1031-1046. 3. Tournier J-D. *et al, ISMRM* 2004:88. 4. Behrens T.E.J. *et al*, *MRM* 2003;50:1077-1088. 5. Armitage *et al*, *Statistical Methods in Medical Research*, Blackwell Publishing, 2001. 6. Alexander D.C. *et al, MRM* 2002;48:331-340.

ACKNOWLEDGEMENTS This work was conducted with the aid of funding by EPSRC and Philips Medical Systems.